Journal of Microscopy, Vol. 171, Pt 2, August 1993, pp. 107–115.
Received 19 October 1992; accepted 10 March 1993

Silver-enhanced colloidal-gold labelling of rabbit kidney collecting-duct cell surfaces imaged by scanning electron microscopy

P. HERTER,* G. LAUBE,* J. GRONCZEWSKI* & W. W. MINUTH†
**Max-Planck-Institut für Molekulare Physiologie, Rheinlanddamm 201, 4600 Dortmund 1, Germany*
†Institute für Anatomie, Universität Regensburg, Universitätsstraße 31, 8400 Regensburg, Germany

Key words. Cell surface, collecting duct, immunogold, lectin, rabbit kidney, scanning electron microscopy, silver enhancement.

Summary

The luminal cell surfaces of rabbit kidney cortical collecting-duct cells were labelled with peanut lectin (PNA) and investigated by scanning electron microscopy. Labelling was performed either on 20-μm-thick cryostat sections from prefixed and cryoprotected rabbit kidney tissue or on cultured collecting-duct epithelium using biotinylated PNA and a 6-nm colloidal-gold-coupled antibody against biotin. Colloidal-gold labels were detected at low magnification (2000–4000×) using silver enhancement. Coating with chromium allowed simultaneous imaging of both cell-surface morphology and labelling topography in the backscattered electron imaging mode. Our results show that PNA binding is specific for a subtype of intercalated cells equipped with microvilli on the luminal surface. The presented method promises to be useful for the identification of specific cell types in heterogeneous tissues.

Introduction

The cortical collecting duct of rabbit kidney consists of morphologically and functionally different cell types: principal cells and intercalated cells. Principal cells are known to reabsorb sodium and secrete potassium (Koeppen *et al.*, 1983). The intercalated cells are involved in the renal regulation system of the acid-base state (Madsen & Tisher, 1983, 1984; Verlander *et al.*, 1987; Brown *et al.*, 1988a, b; Ridderstrale *et al.*, 1988; Schwartz *et al.*, 1988; Alper *et al.*, 1989; Brown, 1989; Satlin & Schwartz, 1989; Schuster, 1990; Wingo *et al.*, 1990; Madsen *et al.*, 1991). They have been divided into proton-secreting A cells and bicarbonate-secreting B cells. As shown previously by scanning electron microscopy (SEM) investigations the intercalated cells display various cell-surface morphologies (Le Furgey & Tisher, 1979). Four different surface patterns of the intercalated cells were described in rabbit kidney (1) intercalated cells with numerous short microvilli; (2) intercalated cells with both short and long microvilli; (3) intercalated cells with microfolds; (4) inter-calated cells with a combination of microvilli and micro-folds. In addition, we found intercalated cells with microvilli cross-linked by a dense surface coat (Herter *et al.*, 1991).

For light microscopical observations lectin labelling is an established tool for the detection of distinct elements in complex tissues or for the identification of specific cell types. In rabbit kidney, for example, fluorescein-conjugated *Dolichos biflorus*–agglutinin (DBA) stains the entire collecting duct (Le Hir & Dubach, 1982), whereas peanut agglutinin (PNA) is selective for only one cell type, the HCO_3^--secreting intercalated B cell in the cortical collecting duct (Le Hir *et al.*, 1982; Schwartz *et al.*, 1985). Double fluorescence labelling experiments using PNA and monoclonal antibodies against principal cells (Gilbert *et al.*, 1990) allowed further discrimination of the different cell types of the cortical collecting duct at the light microscopical level. However, using light microscopy, it is not possible to differentiate the cell types by morphological features in combination with labelling properties. Although SEM proved to be a suitable tool for imaging the different collecting-duct cell types, the correlation of PNA labelling with surface morphology has not yet been shown. Thus, we investigated the morphological features of the PNA-positive intercalated cells in mature rabbit collecting duct and compared it with neonatal rabbit collecting-duct cells kept in culture.

Materials and methods

Fixation of tissue samples

Kidneys of male White New Zealand rabbits (3–4 kg), anaesthetized with chloralhydrate/urethan, were fixed by

retrograde perfusion according to Maunsbach (1966) with a solution containing 2% paraformaldehyde, 2% polyvinylpyrrolidone and 0·02% glutaraldehyde in phosphate-buffered saline (PBS). Small sectors of kidney tissue containing the cortical and outer medullary zone were isolated, cryoprotected in an ascending series of glycerol (1 h in 10%, 1 h in 20% and 1 h in 30%), and finally mounted onto a cork holder and frozen by plunging into liquid propane.

Collecting duct cells in culture

Thin cortical explants from the kidney of newborn New Zealand rabbits were mounted on sterile cell holder sets and placed in 24-well tissue culture plates (Falcon, Becton Dickinson, Heidelberg, Germany). The explants consisted of a piece of capsula fibrosa with adherent collecting-duct ampulla, S-shaped bodies and nephrogenic blastema (Minuth, 1987). During culture of these explants in Iscove's modified Dulbecco's medium (IMDM/HEPES; Gibco-BRL Life Technologies, Germany) containing 10% fetal calf serum, we observed growth of cells from the collecting-duct ampulla. Within 24 h of culture the entire surface of the explant was completely covered by a single layer of collecting-duct epithelium. Preculture was carried out in a Heraeus tissue incubator (Hanau, Germany) at 37°C, in a humified atmosphere containing 5% CO_2/95% air.

To mimic the *in vitro* situation of the kidney, cell cultures were maintained with permanent superfusion of fresh medium (Minuth *et al.*, 1992a,b). The perfusion cell culture was started by mounting the working line, consisting of two bottles and a specific cell culture container (Minucells and Minutissue, Bad Albach, Germany). The cell holder sets with the collecting-duct epithelium were placed in the cell culture container with sterile forceps. The container is placed on a 37°C heating plate and connected to a continuous medium supply of 1 ml/h by a roller pump. IMDM/HEPES was used as the basal control medium; aldosterone (1×10^{-7} M), arginine vasopressin (1×10^{-6} M) and insulin (1×10^{-6} M) were added in various combinations to the different experimental series. All hormones were obtained from Sigma (Deisenhofen, Germany). The superfusion of cultures with medium and the application of the different hormones was started 24 h after preparing the cultures. Total culture time was 14 days (1 day of preculture, 13 days of perfusion culture). Finally, the cultured cells were fixed for 30 min with 2% paraformaldehyde and 0·02% glutaraldehyde in PBS.

Labelling

Labelling was performed on tissue sections and on cultured collecting-duct epithelia according to the following incubation protocol (modified from Tommassen *et al.*, 1985). Cryostat sections 20 μm thick were mounted by thawing on gelatin-coated Thermanox slides. The following incubation protocol for PNA labelling was used.

1 Treat with PBS–glycine (50 mM glycine in PBS) for 15 min.
2 Wash twice with PBG (0·2% gelatine and 0·5% BSA in PBS) for 10 min.
3 Treat with biotinylated PNA, diluted 1 : 20 in PBG-C (0·2% gelatine and 0·5% BSA-C in PBS), for 1 h.
4 Wash twice with PBG.
5 Treat with goat–anti-biotin 6-nm gold conjugate, diluted 1 : 20 in PBG-C, for 1 h.
6 Wash twice with distilled water.
7 Postfix for 5 min in 2% glutaraldehyde in PBS.
8 Silver enhancement for 5 min.
9 Wash twice with distilled water.

A commercially available silver-enhancing kit (Aurion) was used which consisted of two components, initiator and enhancer. Equal proportions of both components were mixed shortly before application. For light microscopical investigations a silver-enhancement time of 20 min was employed. Fluorescence labelling was performed using PBS–glycine and PBG for blocking unspecific binding sites, followed by a 30-min incubation with PNA/FITC diluted 1 : 50 in PBG.

Biotinylated PNA and FITC-coupled PNA were obtained from Sigma, and BSA-C, goat–anti-biotin gold and the silver-enhancement system were obtained from Aurion.

For control experiments the lectin–biotin incubation step was omitted.

Dehydration

PNA-labelled samples, either sections on thermanox-slides or cultured collecting-duct cells on the capsula fibrosa, were dehydrated in an ascending ethanol series and then critical-point dried.

Coating

For SEM investigations the dried tissue sections were coated with 20 nm of carbon by electron-gun evaporation using a Balzers BAF 300 coating unit.

Cultured cells were sputter-coated with a 3-nm chromium layer using the sputter device of a Balzers SCU 020.

Scanning electron microscopy

Samples were studied with an Hitachi S-800 SEM equipped with an annular single-crystal backscattered electron detector (Autrata *et al.*, 1986). The cell-surface morphology of tissue sections was imaged by secondary electrons (SE). The corresponding distribution of silver-enhanced colloidal-gold labels was detected by back-

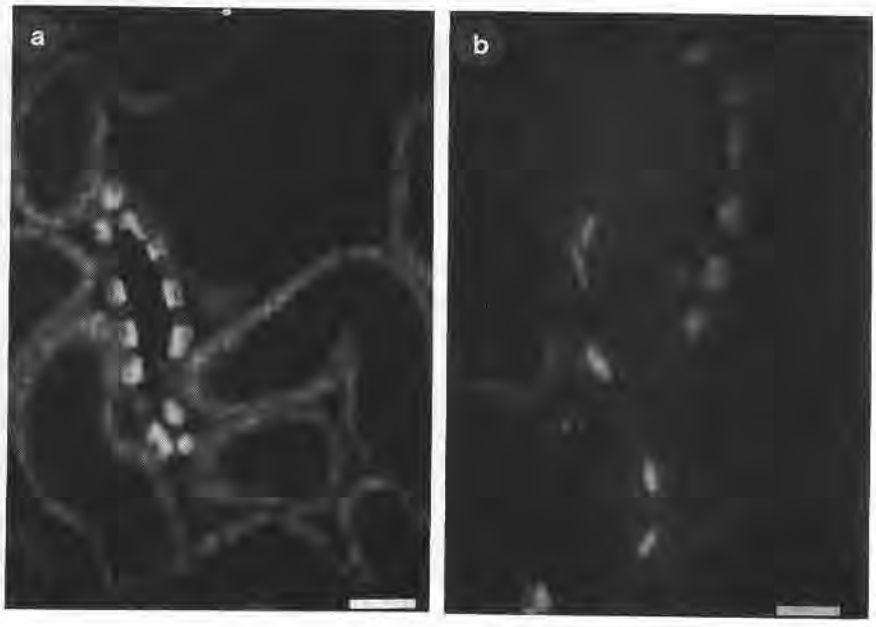

Fig. 1. PNA-labelled cryostat sections imaged by light microscopy. Identification of B cells by (a) biotinylated PNA and anti-biotin–FITC (scale bar = 30 μm) and (b) biotinylated PNA and anti-biotin–gold (6-nm), followed by silver enhancement (epipolarization) (scale bar = 20 μm).

scattered electrons (BE). BE and SE images were recorded from the same scanned area at an accelerating voltage of 10 kV. Chromium-coated cultured cells were exclusively imaged with backscattered electrons. The working distance was 10 mm.

Results

Light microscopical investigations of PNA/FITC-labelled cryosections from rabbit kidney revealed the typical staining pattern of PNA labelling in the cortical collecting duct: only intercalated B cells are labelled (Fig. 1a). Similar results were obtained using biotinylated PNA and a 6-nm gold-conjugated antibody against biotin as a marker (Fig. 1b).

SEM investigations of rabbit kidney cortical collecting duct revealed the characteristic pattern of principal cells and interspersed intercalated cells (Fig. 2a). These cell types could be easily distinguished by their surface morphology. Principal cells showed a smooth apical membrane surface with a relatively few short and stubby microvilli and a single central cilium. In contrast, most of the intercalated cells were equipped with numerous, densely packed microvilli (Fig. 2a). In contrast, a smaller number of these cells exhibited a few sparsely arranged microvilli. On rare occasions the microvilli of intercalated cells were cross-linked by a fibrous surface coat. In addition to these cells with microvilli, a portion of intercalated cells (< 30%) displayed microfolds on their luminal surface. Intercalated cells with a combination of microvilli and microfolds were seldom present.

The heterogeneous composition of the luminal cortical collecting-duct surface is shown by an SE image (Fig. 2a). A principal cell can be identified by its single cilium and flat surface, in contrast to the surrounding intercalated cells, which are equipped with numerous microprojections, such as microfolds or microvilli. The corresponding BE image reveals the distribution of PNA-binding sites labelled by silver-enhanced colloidal gold (Fig. 2b). Distinct labelling was observed on the luminal surface of all intercalated cells covered with microvilli, whereas intercalated cells equipped with microfolds and principal cells are not labelled. The distribution of gold labels on intercalated cells imaged at higher magnifications suggests predominant labelling of the microvilli (Fig. 2c, d). In contrast, the intercalated cells of the collecting duct in the outer medulla showed no labelling, indicating that in this zone only A cells are present.

BE imaging, after coating rabbit kidney collecting-duct cells in culture with chromium, revealed both the cell-surface morphology and corresponding labelling. Figure 3(a) shows an overview of a portion of the cultured cell monolayer at a primary magnification of 2000×. The cells are forming a confluent monolayer. Dark cells alternate with cells exhibiting a bright surface.

The border region between two different cells is illustrated in Fig. 3(b) at a primary magnification of 10 000×. The dark cell on the right-hand side is covered with few short microvilli and shows no labelling. The neighbouring cell on the left shows intense labelling, which is mainly localized in the densely packed microvilli. This decoration of the cell surface with silver-enhanced colloidal-gold-coupled antibodies against biotin results in a bright signal in the BE contrast, which is dependent upon high-atomic-number elements.

Figure 3(c) gives an overview of the variety of cell types with the monolayer. Cell-specific labelling properties can

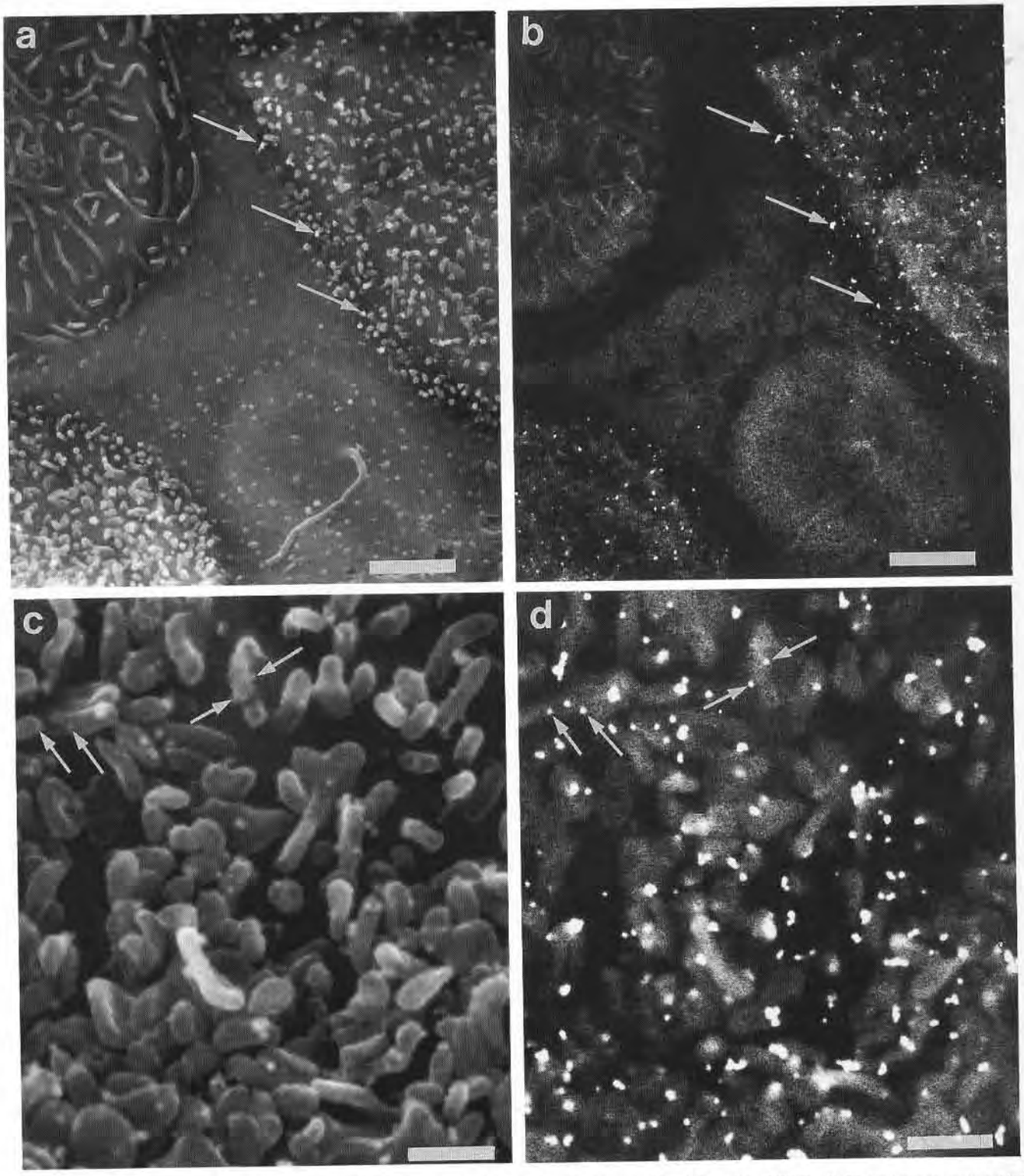

Fig. 2. The luminal surface of PNA–colloidal-gold-labelled cortical collecting duct imaged by SE (a, c) and BE (b, d). The specimen was coated with 20 nm of carbon. (a) Morphology of a principal cell with flat surface and central cilium surrounded by three intercalated cells equipped with microvilli (bottom left, top right) and microfolds (top left). (b) The corresponding distribution of colloidal-gold-labelled PNA binding sites. Arrows in (a) and (b) point to the same colloidal gold particles. Scale bars = 2 μm. (c) Surface morphology and (d) the corresponding distribution of PNA binding sites at a primary magnification of 30 000×. Arrows in (c) and (d) point to the same colloidal gold particles. Scale bars = 0·5 μm.

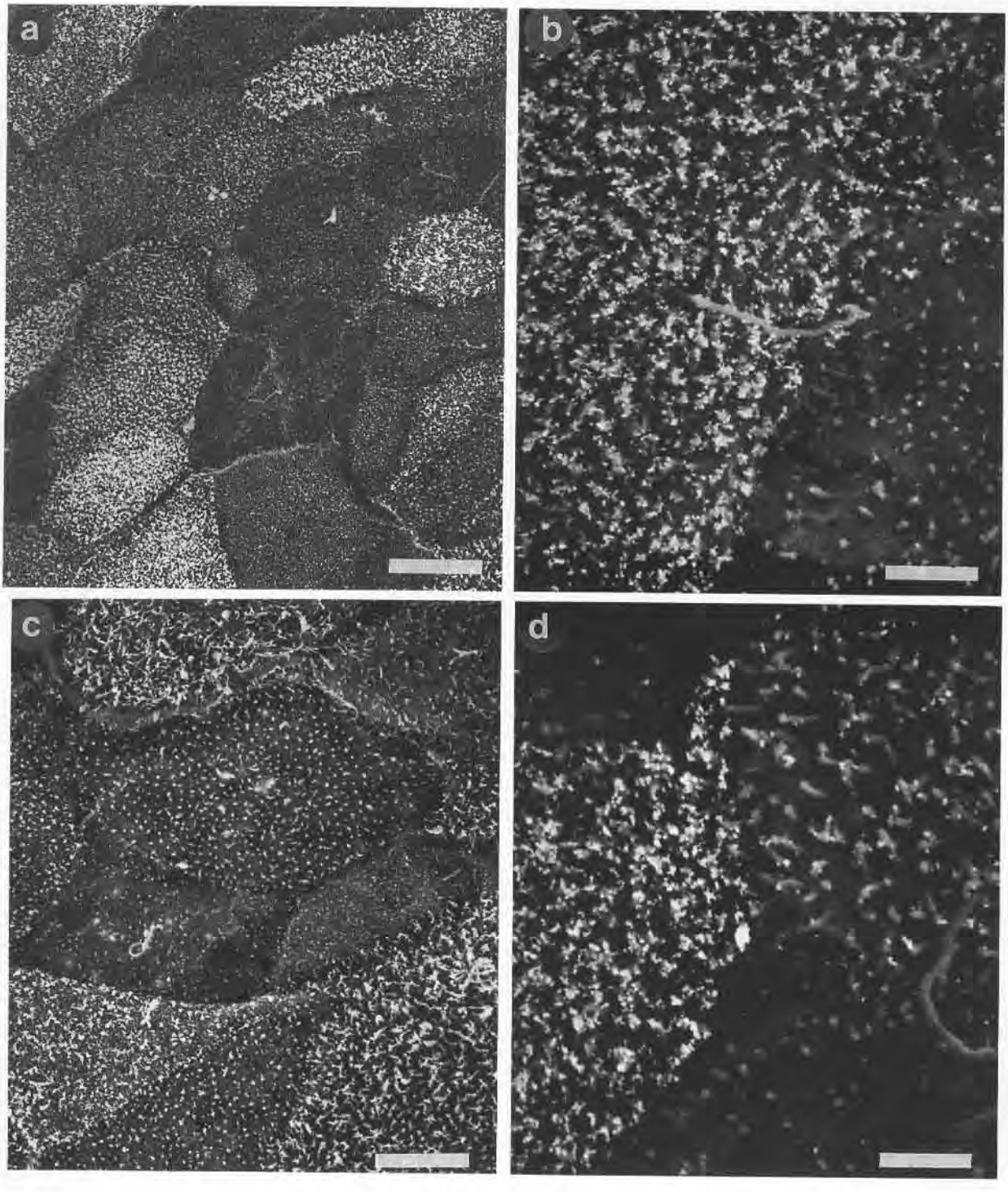

Fig. 3. BE images of cultured collecting-duct epithelium. Specimens were coated with 3 nm of chromium. (a) Overview of the confluent cell monolayer at a low magnification (2000×, scale bar = 7·5 μm). Labelled cells appear bright. (b) Border region of two different cell types. Labelling is clearly visible on the cell on the left-hand side, which is densely covered with microvilli. Labels are predominantly found on the microvilli. The neighbouring cell remained unlabelled (10 000×, scale bar = 1·5 μm). (c) Cultured collecting-duct epithelial cells grown under hormonal influence exhibit a diversity of cell-surface morphologies, which are characterized by the different densities of microvilli (4000×, scale bar = 3·25 μm). (d) Four adjacent cells can be distinguished by their labelling pattern and cell-surface morphology (12 000×, scale bar = 1·25 μm).

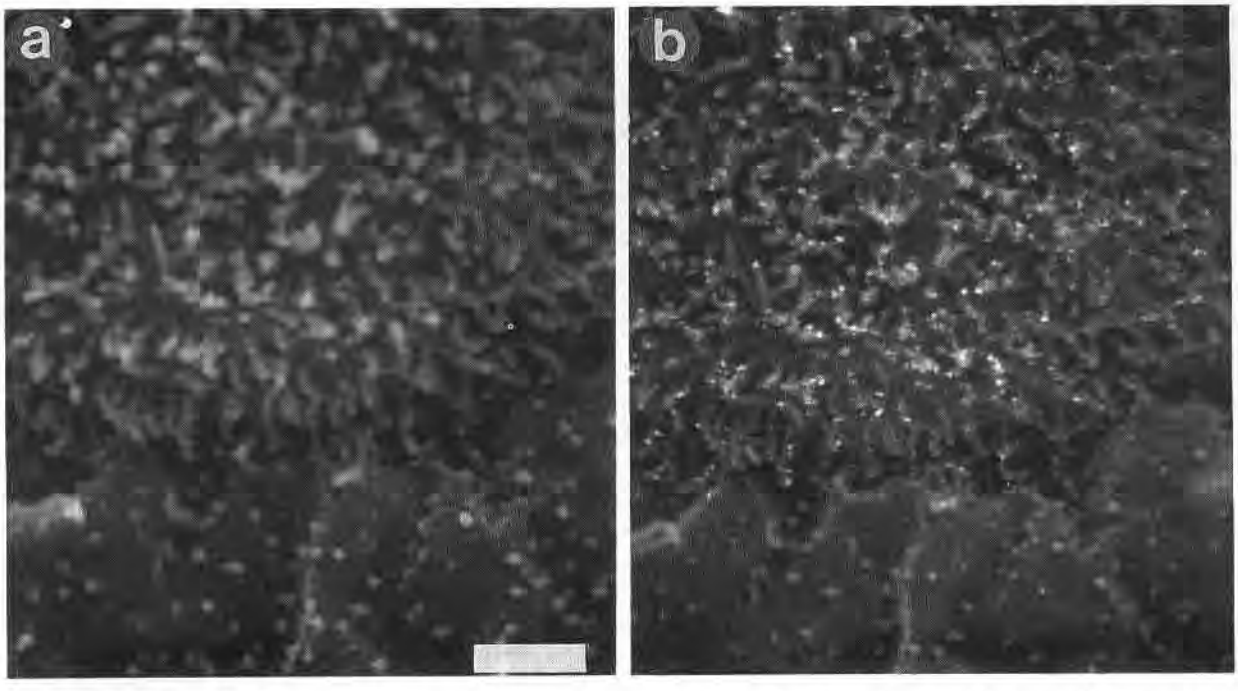

Fig. 4. Comparison of SE and BE images of chromium-coated collecting-duct cells in culture (12 000×, scale bar = 1·25 μm). (a) SE image of two adjacent cell surfaces. The colloidal gold labelling of microvilli on the top cell surface is poor. (b) The same scanned area imaged by BE. The contrast in the BE mode is sufficient to correlate the distribution of gold particles to the morphological details of the cell surface.

already be discerned at a primary magnification of 4000× and become clearer at a magnification of 12 000× (Fig. 3d). Four adjacent cells belonging to three different subtypes can be distinguished by their surface morphology and labelling properties.

No positive staining was observed on tissue or cultured cells when the lectin/biotin incubation step was omitted.

Following hormonal stimulation with aldosterone, insulin and AVP, the cultured collecting-duct epithelia displayed various cell types (Fig. 3c). They could be classified by their surface morphology and density of PNA labelling.

Type 1. Cells with densely packed, short microvilli on the surface. These cells always showed the most intensive labelling, which could be detected clearly even at very low magnifications (2000–4000×).

Type 2. Cells covered with less densely arranged, longer microvilli displayed distinct labelling, especially on the microvilli.

Type 3. Cells with irregularly arranged, thin microvilli showed similar labelling to type 2.

Type 4. Cells exhibiting sparsely arranged, short and stumpy microvilli showed only weak labelling or remained unlabelled.

Type 5. Cells with a smooth surface generally remained unlabelled.

Within this classification many intermediate forms could be found.

Figure 4 shows a comparison of SE and BE imaging at a primary magnification of 12 000×, to prove the quality of both imaging modes when chromium is used as a coating layer. In the SE mode (Fig. 4a) colloidal gold labels on cultured collecting-duct cells can barely be identified, whereas in the BE image of the same scanned area (Fig. 4b) gold labels are clearly visible on the cell surface. In addition, microvilli appear thinner in the BE mode as opposed to the SE mode.

Discussion

The detection of colloidal gold in SEM investigations using the BE imaging mode was introduced by Trejdosiewicz *et al.* (1981). This technique proved to be a suitable tool for the demonstration of cell-surface antigens (Hodges *et al.* 1982, 1987; Walther *et al.*, 1984; Walther & Müller, 1986; Soligo *et al.*, 1987; Namork & Heier, 1988; Pawley & Albrecht, 1988; Stump *et al.*, 1988, 1989; Namork, 1991) and intracellular epitopes (Albrecht *et al.*, 1989; Gross & De Boni, 1990). Using in-lens field-emission SEM, even very small gold particles of about 1 nm can be resolved (Erlandsen *et al.*, 1990; Müller & Hermann, 1990; Hermann *et al.*, 1991). However, there are only a few reports on colloidal-gold labelling of complex tissues composed of morphologically and functionally different cell types (Hodges *et al.*, 1982; Bonvicini *et al.*, 1986; de Harven *et al.*, 1990; Gross & De Boni, 1990). We present a

technique which reveals the distinct labelling of epithelial cell surfaces in kidney tissue.

The collecting-duct epithelium is composed of morphologically and functionally different cell types. Thus far it has not been possible to correlate the PNA binding of collecting-duct cells to the morphological classification. Our approach was to identify unambiguously the PNA-positive cell type within the luminal surface of the cortical collecting duct. In our experience, PNA labelling of large (1–5-mm) tissue specimens turned out to be inefficient, probably because of the low accessibility of binding sites and impaired diffusion of labelling molecules in thick tissue specimens. To overcome these problems, we modified the well-known preparation protocol of fluorescence labelling of cryostat sections for SEM investigations. Labelling was performed on cryostat sections (20 μm thick) exhibiting sufficient areas of luminal surfaces for SEM investigations. Good preservation of structures required the infiltration of the tissue with a cryoprotectant (30% glycerol for 1 h). As demonstrated by the carbon-coated samples in Fig. 2(a, b), distinct gold labels were found on all cells exhibiting microvilli on their luminal surface. Since PNA-positive cells are considered to be B cells (Schwartz *et al.*, 1985, 1988; Schuster *et al.*, 1986), our results suggest that intercalated cells covered with any form of microvilli are B cells, whereas intercalated cells with microfolds are probably A cells. Directly adjacent unlabelled and labelled cells (Fig. 2a, b) show the quality of the labelling specifity.

The numerical proportion and the distribution of A and B cells are influenced by alterations of the acid–base state. Recently, Satlin & Schwartz (1989) found a loss of functional B cells as a result of internalization and degradation of PNA binding in response to an acidic environment. These cellular changes could result in a decrease in the labelling density on the luminal surface of B cells. Regarding this question, lectin gold labelling for SEM may be a suitable technique for the quantitative evaluation of PNA binding sites under the influence of defined physiological conditions.

Investigation of carbon-coated samples means that SE and BE images must be compared. De Harven *et al.* (1984) demonstrated that, on carbon-coated samples, mixing the SE and BE signals provided efficient superposed images of the cell-surface topography and of the colloidal-gold markers. Another approach to avoid dual imaging is to employ a coating layer which yields good contrast in the material-dependent BE signal, without interfering with the signal from the silver-enhanced colloidal-gold labels. This is achieved by coating the samples with a 2–3 nm chromium layer (Fig. 3).

Chromium provides much better BE contrast than carbon (Peters, 1985), i.e. surface structures can be imaged more clearly. Unlike the carbon-coated samples, chromium-coated specimens enable surface structures and colloidal gold labels to be visualized simultaneously in the BE mode because there is a sufficient difference in their atomic numbers (chromium: 24; gold: 79), i.e. gold labels can be easily discerned from structural information. BE imaging of chromium-coated samples reveals finer surface details than SE imaging (Fig. 4). SE imaging reveals only surface structures, and localization of gold labels becomes nearly impossible. BE imaging of chromium-coated samples allows the correlation of colloidal-gold labels to morphological details on the cell surface. Furthermore, cell-surface structures appear finer and thinner in the BE mode. In particular, the difference in the thickness of the microvilli is striking, presumably because SE are generated at the surface of the chromium layer, whereas BE come from the bulk of the chromium layer and the microvilli. The imaging of small colloidal-gold particles (5 nm) requires high primary magnification, above approximately 30 000×. However, at this high magnification the scanned area becomes too small for the identification of specific cell types within the epithelial surface. Brief silver enhancement of the gold labels facilitates the correlation of labelling features of different cell types within a heterogeneous epithelium at low magnification. The use of the silver enhancement system for SEM proposed by Birrell *et al.* (1986), and first applied to single cells (Scopsi *et al.*, 1986) and cytoskeletons (Goode & Maugel, 1987), brings about important advantages. Fast screening of the samples to control the labelling result can be accomplished with light microscopy using epipolarization (Fig. 1b). In SEM the enhanced particle size allows the signal to be detected at low and high magnifications without disturbing the identification of cell types. It is well known that the labelling density decreases with the increasing size of the gold conjugates. Silver enhancement combines high labelling density of small gold particles with an easily detectable BE signal (Namork & Heier, 1988; Hodges & Carr, 1990; Namork 1991).

Our studies of embryonic rabbit collecting-duct cells (Fig. 3) revealed different labelling densities on differentiating cells under defined hormonal influence. Cells were mostly differentiated when aldosterone, insulin and AVP were applied at the same time. The use of specific cell-surface markers in combination with our technique provides a suitable method for the investigation of developmental or functional differentiation processes. The method enables the comparison of *in vivo* and *in vitro* maturation of embryonic to adult tissue.

Acknowledgments

The skilful technical assistance of Carolin Koerner, Marion Kubitza and Jutta Luig is gratefully acknowledged. We also wish to thank Dr Karl Zierold for helpful discussions. The investigation was supported in part by the Deutsche Forschungsgemeinschaft (DFG, Mi 331/2-5).

References

Albrecht, R.M., Prudent, J., Simmons, S.R., Pawley, J. & Choate, J. (1989) Observations of colloidal gold labelled platelet microtubules: high voltage electron microscopy and low voltage–high resolution scanning electron microscopy. *Scanning Microsc.* **3**, 273–278.

Alper, S.L., Natale, J., Gluck, S., Lodish, H.F. & Brown, D. (1989) Subtypes of intercalated cells in rat kidney collecting duct defined by antibodies against erythroid band 3 and renal vacuolar H^+-ATPase. *Proc. Natl. Acad. Sci.* **86**, 5429–5433.

Autrata, R., Walther, P., Kriz, S. & Müller, M. (1986) A BSE-scintillation detector in the (S)TEM. *Scanning*, **8**, 3–8.

Birrell, G.B., Habliston, D.L., Hedberg, K.K. & Griffith, O.H. (1986) Silver-enhanced colloidal gold as a cell surface marker for photoelectron microscopy. *J. Histochem. Cytochem.* **34**, 339–345.

Bonvicini, F., Maltarello, M.C., Versura, P., Bianchi, D., Gasbarrini, G. & Laschi, R. (1986) Correlative scanning electron microscopy in the study of human gastric mucosa. *Scanning Electron Microsc.* **2**, 687–702.

Brown, D. (1989) Membrane recycling and epithelial cell function. *Am. J. Physiol.* **256**, F1–F12.

Brown, D., Hirsch, S. & Gluck, S. (1988a) An H^+ ATPase in opposite plasma membrane domains in kidney epithelial cell subpopulations. *Nature*, **331**, 622–624.

Brown, D., Hirsch, S. & Gluck, S. (1988b) Localization of a proton pumping ATPase in rat kidney. *J. Clin. Invest.* **82**, 2114–2126.

Erlandsen, S.L., Frethem, C. & Autrata, R. (1990) Workshop on high-resolution immunocytochemistry of cell surfaces using field emission SEM. *J. Histochem. Cytochem.* **38**, 1779–1780.

Gilbert, P., Mundel, P. & Minuth, W.W. (1990) Production of monoclonal antibodies against principal cells of the renal collecting duct by in vitro immunization with unsolubilized antigens. *J. Histochem. Cytochem.* **38**, 1919–1925.

Goode, D. & Maugel, T.K. (1987) Backscattered electron imaging of immunogold-labeled and silver enhanced microtubules in cultured mammalian cells. *J. Electron Microsc. Tech.* **5**, 263–273.

Gross, D.K. & De Boni, U. (1990) Colloidal gold labeling of intracellular ligands in dorsal root sensory neurons, visualized by scanning electron microscopy. *J. Histochem. Cytochem.* **38**, 775–784.

de Harven, E., Connolly, J.G., Wang, Y., Hanna, W. & Bootsma, G. (1990) Scanning electron microscopy of immuno-gold labeled antigens associated with bladder cancer. *Scanning Microsc.* **4**, 467–477.

de Harven, E., Leung, R. & Christensen, H. (1984) A novel approach for scanning electron microscopy of colloidal gold-labeled cell surfaces. *J. Cell Biol.* **99**, 53–57.

Hermann, R., Schwarz, H. & Müller, M. (1991) High precision immunoscanning electron microscopy using Fab fragments coupled to ultra-small colloidal gold. *J. Struct. Biol.* **107**, 38–47.

Herter, P., Tresp, G., Hentschel, H., Zierold, K. & Walther, P. (1991) High-resolution scanning electron microscopy of frozen-hydrated and freeze-substituted kidney tissue. *J. Microsc.* **161**, 375–385.

Hodges, G.M. & Carr, K.E. (1990) Colloidal gold immunocytochemistry using SEM. *Eur. Microsc. Anal.* **6**, 17–20.

Hodges, G.M., Smolira, M.A. & Trejdosiewicz, L.K. (1982) Urothelium-specific antibody and lectin surface mapping of bladder urothelium. *Histochem. J.* **14**, 755–766.

Hodges, G.M., Southgate, J. & Toulson, E.C. (1987) Colloidal gold – a powerful tool in scanning electron microscope immunocytochemistry: an overview of bioapplications. *Scanning Microsc.* **1**, 301–318.

Koeppen, B.M., Biagi, B.A. & Giebisch, G.H. (1983) Intracellular microelectrode characterization of the rabbit kidney cortical collecting duct. *Am. J. Physiol.* **244**, F35–F47.

Le Furgey, A. & Tisher, C.C. (1979) Morphology of rabbit collecting duct. *Am. J. Anat.* **155**, 111-124.

Le Hir, M. & Dubach, U.C. (1982) The cellular specificity of lectin binding in the kidney. *Histochemistry*, **74**, 531–540.

Le Hir, M., Kaissling, B., Koeppen, B.M. & Wade, J.B. (1982) Binding of peanut lectin to specific epithelial cell types in the kidney. *Am. J. Physiol.* **242**, C117–C120.

Madsen, K.M. & Tisher, C.C. (1983) Cellular response to acute respiratory acidosis in rat medullary collecting duct. *Am. J. Physiol.* **245**, F670–F677.

Madsen, K.M. & Tisher, C.C. (1984) Response of intercalated cells of rat outer medullary collecting duct to chronic metabolic acidosis. *Lab. Invest.* **51**, 268–276.

Madsen, K.M., Verlander, J.W., Kim, J. & Tisher, C.C. (1991) Morphological adaptation of the collecting duct to acid-base disturbances. *Kidney Int.* **40**, Suppl. 33, S57–S63.

Maunsbach, A.B. (1966) Observation on the segmentation of the proximal tubule in the rat kidney. *J. Ultrastruct. Res.* **16**, 239–258.

Minuth, W.W. (1987) Neonatal rabbit kidney cortex in culture as tool for the study of collecting duct formation and nephron differentiation. *Differentiation*, **36**, 12–22.

Minuth, W.W., Dermietzel, R., Kloth, S. & Hennerkes, B. (1992a) A new method culturing renal cells under permanent superfusion and producing a luminal-basal medium gradient. *Kidney Int.* **41**, 215–219.

Minuth, W.W., Stoeckl, G., Kloth, S. & Dermietzel, R. (1992b) Construction of an apparatus for perfusion cell cultures which enables in vitro experiments under organotypic conditions. *Eur. J. Cell Biol.* **57**, 132–137.

Müller, M. & Hermann, R. (1990) Towards high-resolution SEM of biological objects. *Proc. XIIth Int. Congr. of Electron Microscopy* (ed. by L.D. Peachy and D.B. Williams), Vol. 3, pp. 4–5. San Francisco Press, Inc., San Francisco.

Namork, E. (1991) Double labeling of antigenic sites on cell surfaces imaged with backscattered electrons. *Colloidal Gold: Principles, Methods and Applications* (ed. by M.A. Hayat), Vol. 3, pp. 187–208. Academic Press, Inc., San Diego.

Namork, E. & Heier, H.E. (1988) Silver enhancement of single and double immunogold labeled cells imaged with backscattered electrons. *Proc. IXth Eur. Congr. on Electron Microscopy* (ed. by H.G. Dickinson & P.J. Goodhew), Vol. 3, pp. 547–548. IOP Publishing Ltd., York.

Pawley, J. & Albrecht, R. (1988) Imaging colloidal gold labels in LVSEM. *Scanning*, **10**, 184–189.

Peters, K.-R. (1985) Working at higher magnifications in scanning electron microscopy with secondary and backscattered electrons on metal coated biological specimens and imaging

macromolecular cell membrane structures. *Scanning Electron. Microsc.* **4,** 1519–1544.

Ridderstrale, Y., Kashgarian, M., Koeppen, B., Giebisch, G., Stetson, D., Ardito, T. & Stanton, B. (1988) Morphological heterogeneity of the rabbit collecting duct. *Kidney Int.* **34,** 655–670.

Satlin, L.M. & Schwartz, G.J. (1989) Cellular remodeling of HCO_3-secreting cells in rabbit renal collecting duct in response to an acidic environment. *J. Cell Biol.* **109,** 1279–1288.

Schuster, V.L. (1990) Organization of collecting duct intercalated cells. *Kidney Int.* **38,** 668–672.

Schuster, V.L., Bonsib, S.M. & Jennings, M.L. (1986) Two types of collecting duct mitochondria-rich (intercalated) cells: lectin and band 3 cytochemistry. *Am J. Physiol.* **251,** C347–355.

Schwartz, G.J., Barasch, J. & Al-Awqati, Q. (1985) Plasticity of functional epithelial polarity. *Nature,* **318,** 368–371.

Schwartz, G.J., Satlin, L.M. & Bergmann, J.E. (1988) Fluorescent characterization of collecting duct cells: a second H^+-secreting type. *Am. J. Physiol.* **255,** F1003–1014.

Scopsi, L., Larsson, L.-I., Blastholm, L. & Hartvig Nielsen, M. (1986) Silver-enhanced colloidal gold probes as markers for scanning electron microscopy. *Histochemistry,* **86,** 35–41.

Soligo, D., Lambertenghi-Deliliers, G. & de Harven, E. (1987) Immuno-scanning electron microscopy of normal and leukemic leukocytes labeled with colloidal gold. *Scanning Microsc.* **1,** 719–725.

Stump, R.F., Pfeiffer, J.R., Schneebeck, M.C., Seagrave, J.C. & Oliver, J.M. (1989) Mapping gold-labeled receptors on cell surfaces by backscattered electron imaging and digital image analysis: studies of the IgE receptor on mast cells. *Am. J. Anat.* **185,** 128–141.

Stump, R.F., Pfeiffer, J.R., Seagrave, J.C. & Oliver, J.M. (1988) Mapping gold-labeled IgE receptors on mast cells by scanning electron microscopy: receptor distributions revealed by silver enhancement, backscattered electron imaging, and digital image analysis. *J. Histochem. Cytochem.* **36,** 493–502.

Tommassen, J., Leunissen, J., van Damme-Jongsten, M. & Overduin, P. (1985) Failure of E. coli K-12 to transport PhoE-LacZ hybrid proteins out of the cytoplasm. *EMBO J.* **4,** 1041–1047.

Trejdosiewicz, L.K., Smoira, M.A., Hodges, G.M., Goodman, S.L. & Livingstone, D.C. (1981) Cell surface distribution of fibronectin in cultures of fibroblasts and bladder derived epithelium: SEM-immunogold localization compared to immunoperoxidase and immunofluorescence. *J. Microsc.* **123,** 227–236.

Verlander, J.W. Madsen, K.M. & Tisher, C.C. (1987) Effect of acute respiratory acidosis on two populations of intercalated cells in rat cortical collecting duct. *Am. J. Physiol.* **253,** F1142–F1156.

Walther, P., Kriz, S., Müller, M., Ariano, B.H., Brodbeck, U., Ott, P. & Schweingruber, M.E. (1984) Detection of protein A gold 15 nm marked surface antigens by backscattered electrons. *Scanning Electron Microsc.* **3,** 1257–1266.

Walther, P. & Müller, M. (1986) Detection of small (5–15 nm) gold-labeled antigens using backscattered electrons. *The Science of Biological Preparation for Microscopy and Microanalysis* (ed. by M. Müller, R.P. Becker, A. Boyde and J.J. Wolosewick), pp. 195–201. Scanning Electron Microscopy Inc., AMF O'Hare, Chicago.

Wingo, C.S., Madsen, K.M., Smolka, A. & Tisher, C.C. (1990) H-K-ATPase immunoreactivity in cortical and outer medullary collecting duct. *Kidney Int.* **38,** 985–990.